

# Subarrays of phased-array antennas for multiple-input multiple-output radar applications

Syahfrizal Tahcfulloh<sup>1</sup>, Muttaqin Hardiwansyah<sup>2</sup>

<sup>1</sup>Department of Electrical Engineering, Universitas Borneo Tarakan, Tarakan, Indonesia

<sup>2</sup>Department of Electrical Engineering, Universitas Trunojoyo Madura, Bangkalan, Indonesia

## Article Info

### Article history:

Received Dec 24, 2021

Revised Jul 24, 2022

Accepted Aug 9, 2022

### Keywords:

Amount of detected targets

Angular resolution

Detection probability

SNR detector

Subarray MIMO radar

Virtual array

## ABSTRACT

The subarray MIMO radar (SMIMO) is a multiple-input multiple-output (MIMO) radar with elements in the form of a sub-array that acts as a phased array (PAR), so it combines at the same time the key advantage of the PAR radar, which is high directional gain to increase target range, and the key advantage of the MIMO radar, i.e., high diversity gains to increase the maximum number of detected targets. Different schemes for the number of antenna elements in the transceiver zones, such as uniform and/or variable, overlapped and non-overlapped, significantly determine the performance of radars as virtual arrays (VARs), the maximum number of detected targets, the accuracy of target angle, detection resolution, SNR detection, and detection probability. Performance is also compared with the PAR, the MIMO, and the phased MIMO radars (PMIMO). The SMIMO radar offers great versatility for radar applications, being able to adapt to different shapes of the multiple targets to be detected and their environment. For example, for a transmit-receive with an antenna element number, i.e.,  $M=N=8$ , the range of the number of detected targets for the SMIMO radar is flexible compared to the other radars. On the other hand, the proposed radar's signal-to-noise ratio (SNR) detection performance and detection probability ( $K=5$ ,  $L=3$ ) are both 1,999 and above 90%, which are better than other radars.

*This is an open access article under the [CC BY-SA](#) license.*



## Corresponding Author:

Syahfrizal Tahcfulloh

Department of Electrical Engineering, Universitas Borneo Tarakan

No.1, Jl. Amal Lama No. Kel, Pantai Amal, Tarakan Tim., Kota Tarakan, Kalimantan Utara, Indonesia

Email: rizalubt@gmail.com

## 1. INTRODUCTION

Along with the development of multi-antenna systems on radar technology that detects multiple targets at a long distance, it has a detection function and a flexible response to the target state and its surroundings, supported by high detection accuracy and angle resolution. One of the most important factors in radar performance is optimal range and tracking angle [1] and multi-target detection [2]. High accuracy enhances the ability to detect targets, and high angle resolution increases the number of detected targets. Its implementation requires a radar with high detection accuracy and angle resolution for multiple target detection, especially as an automotive radar [3]. The phased array (PAR) and multiple-input multiple-output (MIMO) radars are two common types of multi-antenna radar systems. This array on the radar system is arranged in order to get a high directivity main lobe [4], [5]. The PAR radar is that all antenna elements are fed by adjusting the phase difference to provide higher directional gain in certain directions only [6], [7], so that the number of detected targets is limited by the small resolution of the resulting angle. The number of detected targets is increased by applying the MIMO radar because it exploits all orthogonal transmission signals to obtain multiple echo signals reflected by multitarget [8]–[11], but has a low directional gain.

Besides, the MIMO system concept has been known to have the advantage of increasing the channel capacity [12], which is directly proportional to the number of detected targets.

The troubles skilled via way of means of the PAR and the MIMO radars are triumph over via way of means of the phased MIMO radar (PMIMO) [13]–[16] via way of means of forming overlapped subarrays (SAs) at the transmit array side (Tx) in order that this radar can concurrently take gain of the primary gain of the PAR radar, specifically excessive directional advantage and the primary gain of the MIMO radar is excessive range advantage to growth the range of goal detection and range. Furthermore, this radar is referred to as PMIMO\_Tx.

In the [17]–[19] study of full PMIMO radar (FPMIMO), using SAs that overlap both Tx and Rx actually yielded the maximum amount of detected targets and angle resolution. It turned out to increase. The amount of SA elements in Tx-Rx array is the same. This radar is also known as the PMIMO\_Tx\_Rx.

To achieve generalization and flexibility of multi-target detection and high angle resolution, this paper introduces the subarray MIMO radar (SMIMO), which allows SAs to have the following conditions: a) the numeral of SA elements varies and or uniform and b) overlapped and or non-overlapped, on Tx-Rx so that it can form a PAR, MIMO, PMIMO\_Tx, PMIMO\_Tx\_Rx radar configuration, and other radar variations. SMIMO radar sub-array conditions provide increased degrees of freedoms (DoFs) compared to other radar types where traditional radars cannot provide detection accuracy, high angle resolution, high SNR detection, and high detection probability to adapt to current environmental conditions. While using the SMIMO radar, all you have to do is adjust the configuration and number of Tx-Rx SAs.

The proposed radar performance is expressed in terms of the number of VAs ( $N_{VAR}$ ), the maximum amount of detected targets ( $\gamma_{max}$ ), the angle resolution, the maximum complex amplitude of the target return, the SNR detection ( $\gamma$ ), and the probability detection ( $P_d$ ). All of these have not been explained in detail in previous studies and have not been shown comprehensively. The results of this paper show that the SMIMO radar is highly flexible in various configurations by adjusting the amount of SA elements, the amount of SAs, overlapped/non-overlapped, and target detection conditions at that time.

The structure of this paper is as follows. In section 2 shows the SMIMO radar system and signal model. The formulas used to calculate  $N_{VAR}$ ,  $\gamma_{max}$ , the magnitude of the complex amplitude,  $\gamma$ , and  $P_d$  are described in section 3. Section 4 presents the results and considerations in the form of numerical calculations and simulations of the SMIMO radar performance parameters, as well as their analysis and verification. Finally, section 5 contains the conclusions of this research.

## 2. THE SMIMO RADAR

### 2.1. System model

The multi-antenna uniform linear array (ULA) radar system in Tx-Rx array consists of a total of  $M$  and  $N$  elements, respectively. The distances between the antenna elements of Tx and Rx array are  $d_M$  and  $d_N$ , respectively. The transmitted signal has a non-dispersive and narrowband propagation. As shown in Figure 1, the Tx and Rx arrays are divided into the numeral of SAs, i.e.  $K$  and  $L$ . These SAs may follow a combination of overlapped and/or non-overlapped, and the numeral of elements may vary. The SA numbers for Tx and Rx are  $1 \leq K \leq M$  and  $1 \leq L \leq N$ , respectively.

Since each SA of both the Tx array and the Rx array acts as an element of the MIMO radar array that acts as a directional gain controller like a PAR radar, the subarray acts as an orthogonal Tx-Rx element of the SMIMO radar and independent of each other. The configuration of these sub-arrays promises a combination of directional gain and diversity gain that can be used simultaneously with both the MIMO and the PAR radars.

Figure 1 shows some configurations (such as overlapped and/or non-overlapped) of various SAs within a Tx-Rx array on a SMIMO radar, and the amount of elements in each subarray that are equal and/or variable. Figure 1(a) shows a proposed radar scheme called a SA in which the SA terms overlap and the numeral of elements in each sub-array is equal (OES), or  $K=3$  and  $L=4$  overlap in Tx and Rx. This configuration detects multiple targets by generating three quadrature signals transmitted by three SAs on Tx and received by four SAs operating independently on Rx. Figure 1(b) shows the conditions between the sub-arrays on the overlapped SMIMO radars, where the amount of elements in each sub-array changes or the overlapping unequal SAs (OUS) with  $K=3$  for Tx and  $L=4$  for Rx. Three orthogonal signals transmitted by the three SAs of Tx and received by the four SAs of Rx. The difference between the OES configuration and the OUS configuration is that the radiation shape (beamforming) of the SAs in the OES configuration is the same for Tx and Rx of each SA, but different for OUS. This is because the OUS configuration has a variable amount of antenna elements, and a SA with many elements produces higher directivity.

The configurations of the proposed radar SAs in Figure 1(c) do not overlap, and each SA has a uniform number of elements (NOES), or Tx has  $K$  sub-arrays and Rx has  $L$  sub-arrays. In this configuration,

for multi-target capture,  $K$  orthogonal signals are generated that are sent by the Tx array and received by the  $L$  independent SAs in the Rx array. Figure 1(d) shows the non-overlapped schemes between the SAs, where the numeral of elements in each sub-array varies or is called a non-overlapping unequal SAs (NOUS), where Tx has  $K$  SAs and Rx has  $L$  SAs. The difference between the NOES configuration and the NOUS configuration is that the sub-arrays with the NOES scheme have the same radial shape for Tx and Rx of each SA, whereas the radial shape for NOUS is different. This is because the NOUS scheme has a variable amount of antenna elements, as described in Figure 1(c). The distinction among overlapped SA (OS) and non-overlapped SA (NOS) is special in section 4.1, i.e. concerning the dimensions of the virtual array (VAR) generated and the sign transmitted through the SAs is semi-orthogonal. This immediately impacts the accuracy and backbone of the detection attitude of the target.

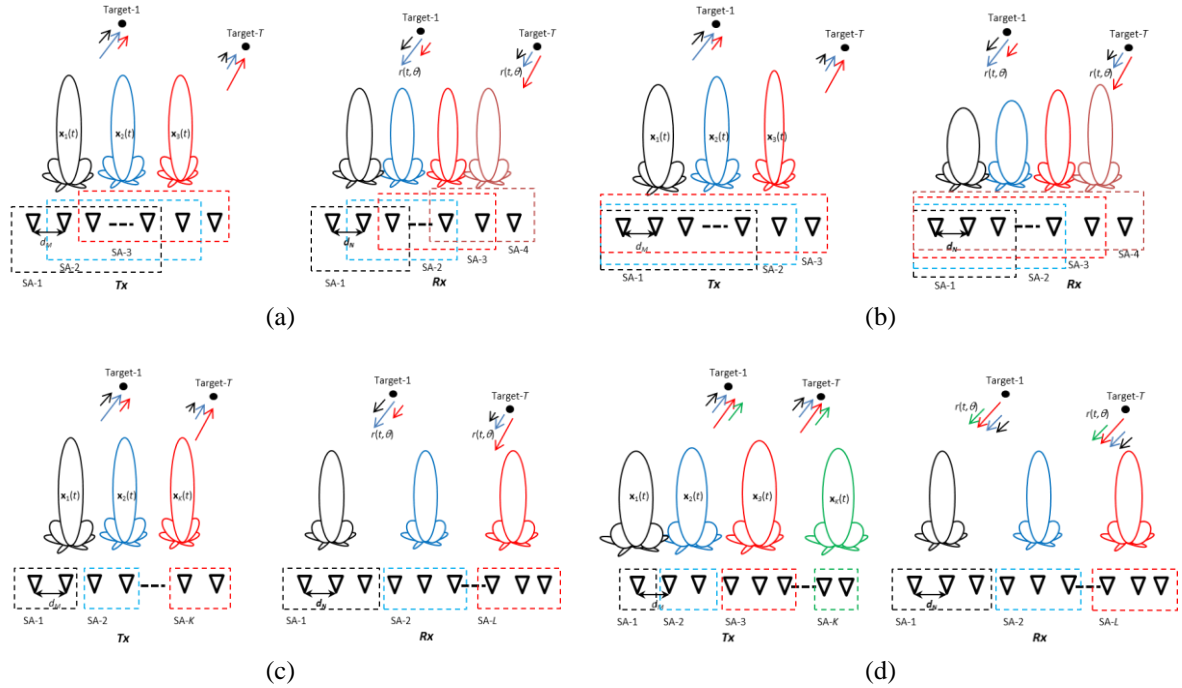


Figure 1. The configuration of the Tx-Rx antenna array on an SMIMO radar with SA is a subarray with the following conditions (a) overlapped-equal number (OES), (b) overlapped-unequal number (OUS), (c) non-overlapped-equal number (NOES), and (d) non-overlapped-unequal number (NOUS)

## 2.2. Signal model

The SMIMO radar block diagram is an adaptation of the PMIMO\_Tx\_Rx radar block diagram described by [18] see Figure 2. The difference lies in the numeral of elements of the SA and the state of the SA, i.e. a non-overlapping number. Tx sub partitions transmit orthogonal signals simultaneously to multiple targets. The  $k$ -th SA of the Tx network sends signals  $\phi_k(t)$  independently of each other. For  $M$  elements in the Tx network, transmit the baseband signal vector through the  $k$ -th SA with  $k=1, 2, \dots, M$ , i.e.

$$x_k(t) = \sqrt{M/K} \phi_k(t) w_k^* \quad (1)$$

where  $(\cdot)^*$  denotes the operator of complex conjugate and  $(M/K)$  is the normalized power factor, ensuring that the energy transmitted by the proposed radar in a pulse is  $M$ . Meanwhile  $w_k$  denotes a complex weight vector of  $M$  unit elements perpendicular to the  $k$ -th SA.

The reflected signal with a reflectance coefficient of  $\beta(\theta)$  from a target  $\theta$  in the distant field is expressed as (2):

$$r(t, \theta) = \sqrt{M/K} \beta(\theta) \sum_{k=1}^K w_k^H a_k(\theta) e^{-j2\pi f \tau_k(\theta)} \phi_k(t) \quad (2)$$

where  $(.)^H$  is the Hermitian displacement operator,  $\mathbf{a}_k(\theta)$  denotes the Tx direction vector with  $M$  elements in the  $k$ -th SA,  $f$  denotes the carrier signal frequency,  $\tau_k(\theta)$  denotes the corresponding delay time of the first element of the  $k$ -th SA to the first element of the first SA.

When the Tx coherent vector and the Tx diversity vector are defined as  $K$ -elements, respectively:

$$\mathbf{c}(\theta) = [\mathbf{w}_1^H \mathbf{a}_1(\theta) \quad \mathbf{w}_2^H \mathbf{a}_2(\theta) \quad \cdots \quad \mathbf{w}_K^H \mathbf{a}_K(\theta)]^T \quad (3)$$

and

$$\mathbf{d}(\theta) = [e^{-j2\pi f \tau_1(\theta)} \quad e^{-j2\pi f \tau_2(\theta)} \quad \cdots \quad e^{-j2\pi f \tau_K(\theta)}]^T \quad (4)$$

So (2) can be stated briefly as

$$\mathbf{r}(t, \theta) = \sqrt{M/K} \beta(\theta) (\mathbf{c}(\theta) \circ \mathbf{d}(\theta))^T \boldsymbol{\psi}(t) \quad (5)$$

where  $(\cdot)^T$  denotes the transpose operator,  $\boldsymbol{\psi}(t) = [\varphi_1(t) \quad \cdots \quad \varphi_K(t)]^T$  and  $\circ$  denotes the operator of Hadamard multiplication. If it is assumed that there are  $T$  targets in the direction  $\{\theta_t\}$  with  $t=1, 2, 3, \dots, T$ , then the complex of signal received vector by the sub-array  $L$  at Rx is:

$$\mathbf{y}(t) = \sqrt{M/K} \sum_{t=1}^T \beta_t(\theta_t) [\mathbf{e}(\theta_t) \circ \mathbf{f}(\theta_t)] [\mathbf{c}(\theta_t) \circ \mathbf{d}(\theta_t)]^T \boldsymbol{\psi}(t) + \mathbf{n}(t) \quad (6)$$

with

$$\mathbf{e}(\theta) = [\mathbf{v}_1^H \mathbf{b}_1(\theta) \quad \mathbf{v}_2^H \mathbf{b}_2(\theta) \quad \cdots \quad \mathbf{v}_L^H \mathbf{b}_L(\theta)]^T \quad (7)$$

and

$$\mathbf{f}(\theta) = [e^{-j2\pi f \tau_1(\theta)} \quad e^{-j2\pi f \tau_2(\theta)} \quad \cdots \quad e^{-j2\pi f \tau_L(\theta)}]^T \quad (8)$$

where  $\mathbf{b}_l(\theta)$  denotes the Rx steering vector with  $N$  elements in the  $k$ -th sub-array and  $\mathbf{v}_l$  is the complex weight vector with  $N$ -unit elements in the  $l$ -th sub-array. Meanwhile  $\mathbf{e}(\theta)$  and  $\mathbf{f}(\theta)$  are the Rx coherent vectors and the Rx diversity vectors with  $L$  element and  $\mathbf{n}(t)$  denotes the  $N$  element vectors of zero mean white Gaussian noise.

### 3. VIRTUAL ARRAY, MAXIMUM AMOUNT OF DETECTED TARGETS, COMPLEX AMPLITUDE OF ECHO SIGNAL, SNR DETECTION, AND DETECTION PROBABILITY FOR SMIMO RADAR

The advantage of orthogonally transmitted MIMO radar over the PAR radar is the formation of VAR [11]. Target detection, angular accuracy, detection angle resolution, and maximum numeral of detected targets are primarily determined by the VAR of the PAR and MIMO radar [11] and the FPMIMO radar [19] with evenly overlapping SAs.

VAR calculations at the MIMO, the PAR, the PMIMO\_Tx\_Rx, and the PMIMO\_Tx radars had been supplied through [19], at (14)-(17). For the most wide variety of detectable goals the MIMO and the PAR radars had been mentioned through [20], whilst for the PMIMO\_Tx\_Rx and the PMIMO\_Tx radars it's been mentioned through [19]. The calculation of the angular decision acquired through the complicated amplitude of the goal echo sign at the PMIMO\_Tx\_Rx, the MIMO, the PMIMO\_Tx, and the PAR radars has been defined through [19]. For the SNR detector on the proposed radar is an extension of the SNR detector on the MIMO radar by [21]. Meanwhile, to determine the detection probability on the SMIMO radar, we adapt  $P_d$  from the FPMIMO radar by [19].

The calculation of VAR, the maximum amount of targets that can be detected, and the complex amplitude of the target return signal on the proposed radar is an extension of the study in [19]. The number of both overlapped and non-overlapped SAs, and/or the number of SMIMO radar VARs that vary uniformly or have a number of Tx and Rx SAs, is defined by  $K$  and  $L$ , respectively.

$$E \in [K + L - 1, KL] \quad (9)$$

To calculate the maximum amount of detected targets on the proposed radar is (10)

$$T_{max} \in \left[ \frac{K+L-2}{2}, \frac{KL+1}{2} \right) \quad (10)$$

The complex amplitude of the SMIMO radar target return signal is expressed by (11):

$$\hat{\beta}(\theta) = \frac{\sqrt{M/K} \sum_{q=1}^Q (e(\theta) \circ f(\theta))^H \hat{\mathbf{R}}_{\mathbf{y}\psi}(c(\theta) \circ \mathbf{d}(\theta))^*}{\|e(\theta) \circ f(\theta)\|^2 (c(\theta) \circ \mathbf{d}(\theta))^T \hat{\mathbf{R}}_{\psi\psi}(c(\theta) \circ \mathbf{d}(\theta))^*} \quad (11)$$

with (12) and (13)

$$\hat{\mathbf{R}}_{\mathbf{y}\psi} = (1/Q) \sum_{q=1}^Q \mathbf{y}(q) \boldsymbol{\psi}^H(q) \quad (12)$$

$$\hat{\mathbf{R}}_{\psi\psi} = (1/Q) \sum_{q=1}^Q \boldsymbol{\psi}(q) \boldsymbol{\psi}^H(q) = \mathbf{I}_{M \times M} \quad (13)$$

where  $\|\cdot\|$  is the euclidean norm operator,  $\hat{\beta}(\theta)$  denotes the least squares (LS) estimate of the coefficient reflectivity of radar or the magnitude of the target's complex amplitude in the direction  $\theta$ , and  $q=1, 2, 3, \dots, Q$  denotes the sample data index. The amount of detected targets can be determined from the spatial spectral peaks in the LS estimate.

Through the same approach by [19] and based on the SNR detector by [21], to calculate the SNR detector on the proposed radar is expressed by (14):

$$\gamma = \frac{2(M/K)^2 M_K^2 N_L^2 K^2 L^2 (SNR)^2}{(M/K)^2 M_K^2 N_L^2 K^2 L^2 (SNR)^2 + 2(M/K) M_K N_L K L (SNR) + 2} \quad (14)$$

where  $M_K$  and  $N_L$  are  $M-K+1$  and  $N-L+1$ , respectively.

Meanwhile, to determine the detection probability on the SMIMO radar by developing  $P_d$  in [19] for a certain false alarm probability ( $P_{fa}$ ) and the SNR is expressed by (15):

$$P_d = \exp\left(\frac{K \ln(P_{fa})}{K + M M_K N_L K L (SNR)}\right) \quad (15)$$

## 4. RESULTS AND DISCUSSION

### 4.1. Virtual array

Calculating VAR ( $N_{VAR}$ ) with SMIMO radar allows you to apply the concept of VAR with the MIMO radar. That is, antenna-shaped elements can be used to radiate orthogonal signals and extend to subarray-shaped elements that are not mutually exclusive overlaps or NOES. VAR is the result of the convolution of the Tx array and Rx [11]. To determine the VAR, the subarray is considered a single antenna in the site center and emits orthogonal signals according to the scheme shown in [11]. Based on a comparison with PMIMO\_Tx with 4 OES, the following is an example of VAR calculation for proposed radar with ( $M=N=8$ ) and 4 NOES (2 elements per subarray).

$$\begin{aligned} Tx \text{ Array} &= \{0 \ 1 \ 0 \ \textcolor{red}{1} \ 0 \ \textcolor{green}{1} \ 0 \ \textcolor{blue}{1}\}; Rx \text{ Array} = \{1 \ 1 \ 1 \ 1 \ 1 \ 1 \ 1 \ 1\}; \\ VAR &= \{1 \ 1 \ 2 \ 2 \ 3 \ 3 \ 4 \ 4 \ 3 \ 3 \ 2 \ 2 \ 1 \ 1 \ 0\} \end{aligned} \quad (16)$$

Since there are four NOES, there is one compelling element position that is displayed in different font colors. The Rx array is worth one in the position of eight elements. The VAR of the SMIMO radar using NOES is 14, which is near to the VAR amount of the MIMO radar of 15. For comparison of SMIMO radar using 2 NOES (numeral of elements per 4 SAs).

$$\begin{aligned} Tx \text{ Array} &= \{0 \ 0 \ 0 \ \textcolor{red}{1} \ 0 \ 0 \ 0 \ \textcolor{green}{1}\}; Rx \text{ Array} = \{1 \ 1 \ 1 \ 1 \ 1 \ 1 \ 1 \ 1\}; \\ VAR &= \{0 \ 1 \ 1 \ 1 \ 1 \ 2 \ 2 \ 2 \ 2 \ 1 \ 1 \ 1 \ 0 \ 0\} \end{aligned} \quad (17)$$

then the VAR variety for the SMIMO radar with 2 NOES is 13.

For the PMIMO\_Tx radar pronounced by [13] which makes use of a radiation detail withinside the shape of Tx OES, in accordance to [11] every waveform is radiated from the midpoint of the segment or the vicinity of the antenna detail withinside the SA with  $M_K$  the maximum middle detail can be 1 at the same time as the others are 0. Here are a few examples of VAR calculations for the PMIMO\_Tx radar with the

same amount of Tx-Rx antenna elements. For example, the configuration of  $K$  is four then  $M_K$  is 5. The shape of Tx-Rx array and VAR are:

$$\begin{aligned} Tx \text{ Array} &= \{0 \ 1 \ 1 \ 1 \ 0 \ 0\}; Rx \text{ Array} = \{1 \ 1 \ 1 \ 1 \ 1 \ 1\}; \\ VA &= \{0 \ 1 \ 1 \ 1 \ 1 \ 2 \ 2 \ 2 \ 2 \ 1 \ 1 \ 1 \ 1 \ 0 \ 0\} \end{aligned} \quad (18)$$

Since there are 4 SAs per SA 5, the element in the center of each SA is worth 1, shown in different font colors, and the Rx array is worth 1. There are 8 element positions. The PMIMO radar has a VAR number of 11, which is between two extreme configurations, slightly higher than the PAR radar, i.e. 8, and lower than the MIMO radar, i.e. 15.

To compare the amount of VARs for proposed radar using OES and NOES, Table 1 shows the numeral of OES or NOES type SAs, the amount of elements per SA, the amount of OES and NOES, and the amount of VARs. The numeral of overlapped locations on the SMIMO-OES radar clearly affects the VAR because there are multiple elements between the shared SAs and the signals are not perfectly orthogonal. This is shown in the configuration of two OESs, with six element positions in the O state, where  $N_{VAR}$  is close to  $N_{VAR}$  on the PAR radar i.e. 9. Meanwhile, if the position of the element in state O is small (like the scheme of 7 OES with 1 element in state O),  $N_{VAR}$  will be one or more of  $N_{VAR}$  in the MIMO radar. The OES-based PMIMO\_Tx radars generally have a higher SINR [13] due to the large amount of OES elements, but have a higher of the directional gain, such as the PAR radars [22], [23]. Therefore, a compromise must be made between  $N_{VAR}$  and the amount of OES, which is proportional to the angle resolution, angle accuracy, and the numeral of detected targets, to conform to the situations of the desired target of radar.

Table 1. Comparison of the SMIMO radar with NOES and OES for  $M=N=8$

	Amount of SAs	Amount of elements per SA	Amount of overlapped locations between SAs	Amount of non-overlapped locations between SAs	$N_{VAR}$
NOES	2	4	0	2	13
	4	2	0	4	14
	8	1	0	8	15
OES	2	7	6	2	9
	3	6	5	2	10
	4	5	4	2	11
	5	4	3	2	12
	6	3	2	2	13
	7	2	1	2	14

During the calculation of  $N_{VAR}$  on the FPMIMO/PMIMO\_Tx\_Rx radar reported by [18] and [19], Tx and Rx are OES, and according to [11] each signal is emitted from the midpoint of the phase or the position of the antenna element. The Tx subarray with  $M_K$  has a central element value of 1 and the other elements 0. The same conditions apply to Rx SAs with many elements. That is,  $N_L$ . For example, if you calculate  $N_{VAR}$  with  $K=L=4$  and then  $M_K=N_L$  is 5, the array will be Tx, Rx, and VAR.

$$\begin{aligned} Tx \text{ Array} &= \{0 \ 1 \ 1 \ 1 \ 0 \ 0\}; Rx \text{ Array} = \{0 \ 1 \ 1 \ 1 \ 0 \ 0\}; \\ VAR &= \{0 \ 0 \ 0 \ 0 \ 1 \ 2 \ 3 \ 4 \ 3 \ 2 \ 1 \ 0 \ 0 \ 0\} \end{aligned} \quad (19)$$

In case there are 4 SAs in Tx and Rx array, the arrangement of the elements is alike. The  $N_{VAR}$  of the PMIMO\_Tx\_Rx radar is 7 because out of the 15 slots in the VAR element with a value greater than 1, only 7 are available. The following is a table showing the result  $N_{VAR}$  of all configurations formed for  $K=L=8$  using (9) as shown in Table 2. Table 2 shows that the  $N_{VAR}$  in the SA configuration of proposed radars such as PMIMO\_Tx and PMIMO\_Tx\_Rx is intermediate between the PAR and the  $N_{VAR}$  of the MIMO radar and gives the  $N_{VAR,PAR} < N_{VAR,SMIMO} < N_{VAR,MIMO}$ . These results also show the proposed radar with the numeral of Tx and Rx SAs.  $K$  and  $L$  are common forms of radar that emit many orthogonal signals. Special conditions for proposed radar are the PAR or SMIMO OES radar ( $M=1$ ,  $N=8$ ), the MIMO or SMIMO NOES ( $M=N=8$ ), and the PMIMO\_Tx or SMIMO OES ( $1 < K < M$ ,  $L=8$ ).

However, if  $d_M$  and  $d_N$  are not equal with  $d$  and are greater than  $d$ , the resulting  $N_{VAR}$  will be greater than those tabulated in Table 2. Similarly, for the magnitudes  $d_M=Ld_N$  and  $d_N=d$ , the maximum value of  $N_{VAR}$  becomes  $KL$ . For example, if  $K=L=8$ , the maximum  $N_{VAR}$ s for the PAR, the MIMO, the PMIMO\_Tx, and the PMIMO\_Tx\_Rx radars are 8, 64, 32, and 16, respectively. However, in reality,  $M=N$ , which is already safe. For example, it is not possible programmatically to set the spacing between the elements of Tx and Rx in

order to get the uppercase  $N_{VAR}$ . The antennas on the Tx and Rx arrays are almost always in a specific location from the beginning.

Table 2. The value of  $N_{VAR}$  is of the array Tx-Rx with  $K=L=8$  and  $d_M=d_N$  is  $d$

$N_{VAR}$	$L$							
	1	2	3	4	5	6	7	8
$K$	1	1	2	3	4	5	6	7
	2	2	3	4	5	6	7	8
	3	3	4	5	6	7	8	9
	4	4	5	6	7	8	9	10
	5	5	6	7	8	9	10	11
	6	6	7	8	9	10	11	12
	7	7	8	9	10	11	12	13
	8	8	9	10	11	12	13	14

#### 4.2. Angle resolution

The formation of the VAR is due to the Tx array transmitting the quadrature signal, thus forming a more focused radiation or beam ray. This happens because a large array is formed in the VAR. The output beam scheme is the product of the Tx and the Rx beam scheme. The Tx beam ray is the power pattern radiated from the Tx antenna in all directions of the target. Similarly, the Rx beam ray is the received power pattern from the target as the arrival angle function of the return signal. If the Rx uses only one antenna, it is difficult to determine the arrival of angle as it will be difficult to distinguish between strong signals from the top of the beam and weak signals in the side lobes. However, if Rx is an array, this does not happen and the beam can be digitally directed to the reach angle of the echo signal.

Figure 2(a) shows the MIMO radar beam schemes for a two-element Tx array and a three-element Rx array. The spacing between the Tx and the Rx array elements is  $0.5 \lambda$ . Here,  $\lambda$  is wavelength a carrier signal. Its output beam ray is similar to the Rx beam ray. However, if you increase the spacing among the elements of the Tx array to 3 times  $d_N$ , the resulting beam scheme is shown in Figure 2(b). The resulting beam pattern has a narrower beam width. Also, the grating lobes that appear in the beam scheme do not seem to appear in the output beam ray. The output beam ray in Figure 2(c) is similar to Figure 2(b), with the difference that the spacing between the elements of Tx is  $0.5 \lambda$ , while the spacing between the elements of Rx is twice  $d_M$ . Therefore, the beam ray can also be represented as a pattern from a  $2 \times 3 = 6$  element Rx array, or the output beam ray is a VAR beam scheme as shown in Figure 2(d). This shows that calculating the correct geometry between the correct element of the Tx array and Rx improves the angle resolution of the radar system without adding the element of antenna to the array.

For PAR transmit signals, a high gain beam is obtained and the SNR is increased  $M$ -fold, which does not occur for quadrature signal transmissions. Therefore, it is necessary to find a compromise between signal transmission with directional amplification and quadrature signal transmission in order to obtain angular resolution that meets the target conditions. This guarantees a compromise between the two extreme configurations and supports the application of the proposed radar concept, which can simultaneously provide SNR, angle resolution, maximum amount of detected targets, and beam schemes. The use of SAs is a compromise between Tx-Rx gain, SINR, and maximum range, as described in [22] and [23].

There is capacity for the usage of SAs with extraordinary variety of elements (unequal subarray, US) to triumph over the restrictions of identical subarray (ES). Especially if it's far adjusted to the situations for detecting more than one objectives due to the fact usually with excessive directional benefit it's far appropriate for objectives which have an extended variety and weak or small radar cross section (RCS). If the goal situations range i.e. varies in variety, RCS, etc., then using an aggregate of various SA schemes (OS/NOS and ES/US) may be found out as an example in a single time and one Tx array may be found out as a non-overlapped identical SA (NOES), overlapped identical SA (OES), non-overlapped unequal SA (NOUS), or overlapped unequal SA (OUS). However, there additionally wishes to be technical issues in its implementation which decide whether or not it may be implemented practically, particularly to the waveform generator in Tx and sign processor in Rx for the utility of the SA methods.



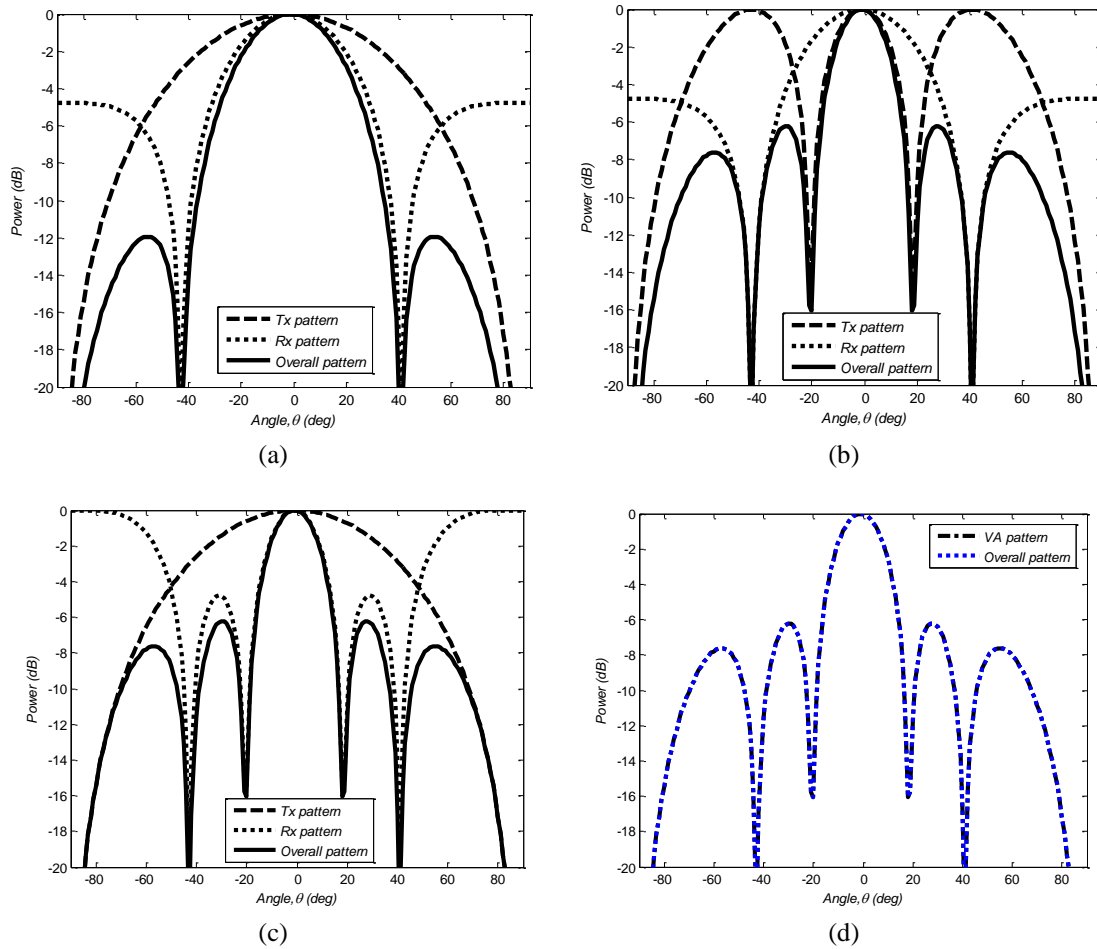


Figure 2. The MIMO radar beam patterns with  $M=2$ ,  $N=3$ , and  $d=0.5\lambda$  for (a)  $d_M=d_N$  is  $d$ , (b)  $d_M=3d$ ,  $d_N=d$ , (c)  $d_M=d$ ,  $d_N=2$ , and (d) VAR and the whole sample

#### 4.3. Relationship between VAR and maximum amount of discoverable targets

Section 4.1 explained the relationship between the numerical calculation of VAR using (9) reported in [20]. Since VAR is proportional to angle resolution and accuracy, it is also proportional to the calculation of the maximum amount of detected targets ( $\gamma_{max}$ ). In calculating the maximum numeral of the MIMO radar targets formulated in [20], at (22), it is also useful to calculate the maximum amount of detected targets for PAR, PMIMO\_Tx, and PMIMO\_Tx\_Rx radars i.e. special conditions for proposed radar. Radar uses (10). To demonstrate this, (11) is used to obtain numerical results as shown in Figure 3. This shows a comparison of these four parameters for all variations of the proposed radar at  $K=4$ ,  $L=5$ , and  $M=N$  is about 8.

As shown in Figure 3, the MIMO and the PMIMO\_Tx radars can detect the four targets indicated by the red dotted vertical lines. That is,  $\theta_D=\{-25^\circ, -10^\circ, 5^\circ, 15^\circ\}$ , but only two the PAR radar and the PMIMO\_Tx\_Rx radars can detect the target.  $\theta=\{-25^\circ, -10^\circ\}$ . MIMO radar has the highest detection accuracy of the four radars. Similarly, it detects the magnitude of the complex amplitude of the return signal most often obtained by MIMO radar. This is related to the amount of VARs in the largest MIMO radar, which improves angle detection accuracy and angle resolution.

Based on the  $\gamma_{max}$  in (10) of the SMIMO radar, the  $\gamma_{max}$  value of the PMIMO\_Tx and PMIMO\_Tx\_Rx radar signal schemes is between the PAR and the  $\gamma_{max}$  value of the MIMO radar, and they are related i.e.  $\gamma_{max,PAR} < \gamma_{max,PMIMO} < \gamma_{max,MIMO}$ . For example, for Tx-Rx with  $K=L$  is 8, get  $\gamma_{max,PAR}$ ,  $\gamma_{max,MIMO}$ ,  $\gamma_{max,PMIMO-Tx}$ , and  $\gamma_{max,PMIMO-Tx-Rx}$ , that is, 4, (7, 32), (5, 16) and (3, 8), respectively. Looking at Figure 3, the MIMO and the PMIMO radars are within the detectability limits of more than four radars, so they can properly detect four targets.



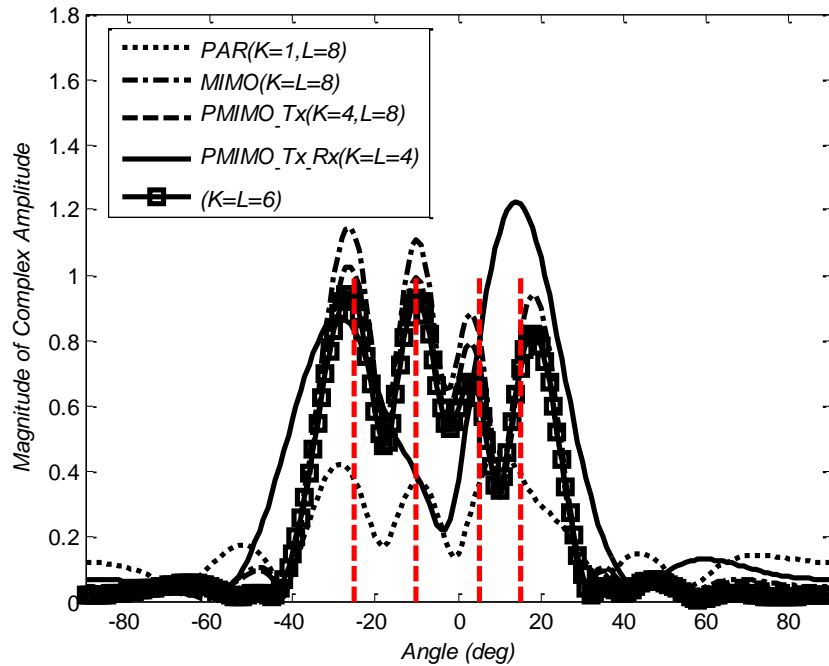


Figure 3. The magnitude of the complex amplitude as an assessment of the accuracy and resolution of the goal attitude with  $\theta_b$  and  $\beta(\theta)=1$  for numerous radar configurations

#### 4.4. SNR detector

The best performance measure of various detectors is  $P_d$  which will be presented in section 4.5. So comparisons of  $P_d$  of various radar systems must be made and selected to determine which one is the best. The comparison is a numerical calculation of a single scalar performance measure such as a function of the detector's SNR performance [21].

Figure 4 is the result of the evaluation of expression (14) to calculate the SNR detector performance of the proposed radar. It is assumed that  $M=N=8$  and the SNR range= $\{-10:1:15\}$  where the radar configurations of the PAR, the MIMO, the PMIMO\_Tx, and two variations of SMIMO are  $(K=1, L=8)$ ,  $(K=L=8)$ ,  $(K=4, L=8)$ ,  $(K=5, L=3)$ , and  $(K=7, L=6)$ , respectively. It appears that the SNR detector of the PAR radar is superior to other radar configurations, especially for low SNR, but when the SNR is above 10 dB, generally the performance of the SNR detector from the proposed radar, namely SMIMO, tends to reach the same value as the SNR detector from the PAR radar. For example, for an SNR condition of 10 dB, the SNR detector constant value ( $\gamma$ ) for PAR, MIMO, PMIMO\_Tx radars, and the two proposed radar variants are 1,998, 1,994, 1,996, 1,999, and 1,995, respectively. The results also show that the variation in the amount of SAs in Tx-Rx, i.e.  $K$  and  $L$ , affects the value of  $\gamma$  where it is evident that the proposed radar configuration  $(K=5, L=3)$  has a high value compared to the special configuration of the proposed radar, namely the PAR radar. Thus, the SMIMO radar has high flexibility to detect multiple targets by adjusting the numeral of Tx-Rx SAs, i.e.  $K$  and  $L$ .

#### 4.5. Detection probability

In the radar detection results according to [21] that the performance of the PAR radar outperforms compared to the MIMO radar at low SNR but the condition is reversed for high SNR. Based on (15) with similar assumptions to the previous evaluation, i.e.  $M=N=8$ , the SNR is set to 10 dB, and the range  $P_{fa}=\{0:0.1:1\}$  where the configurations of the PAR, the MIMO, the PMIMO\_Tx, and the SMIMO radars respectively are  $(K=1, L=8)$ ,  $(K=L=8)$ ,  $(K=4, L=8)$ , and  $(K=L=4)$ , the results are obtained as presented in Figure 5. The numerical evaluation results in Figure 5 corroborate the results discussed in section 4.4 and as reported by [21] namely the  $P_d$  performance of the PAR radar outperforms the performance of other radars. While at a low  $P_{fa}$  of about  $10^{-4}$ , all  $P_d$  performances of the SMIMO radar variation have  $P_d$  values above 90%. This shows that detection target is more-best for SNR values above 10 dB. It also appears that the variation in the amount of SAs in Tx-Rx namely  $K$  and  $L$  affects the  $P_d$  value. This is evident because the PAR, the MIMO, and the PMIMO\_Tx radars are special conditions of the proposed radar.

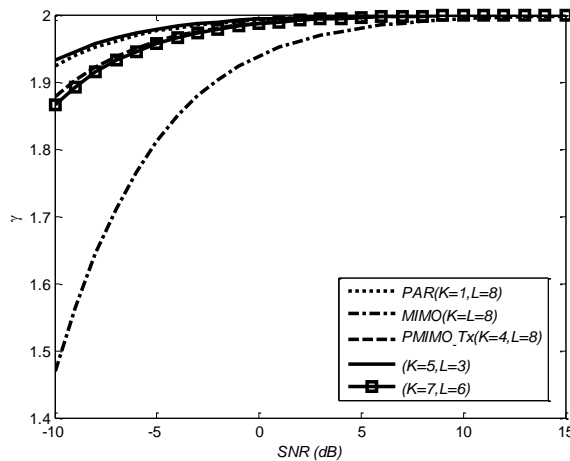


Figure 4. SNR detection of various SMIMO radar configurations for SNR variations

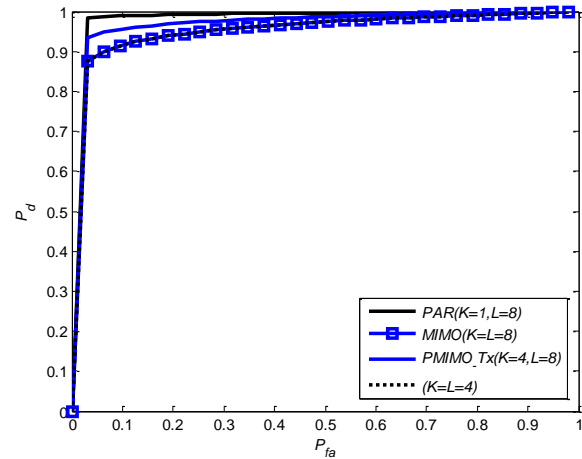


Figure 5. The detection probability for various SMIMO radar configurations for  $P_{fa}$  variations

## 5. CONCLUSION

This article described the number of the VARs, the angle resolution, the maximum number of detectable targets, the magnitude of the complex amplitude, the SNR detector, and the detection probability of the SMIMO radar return signal under various SA configurations. The number of VARs strongly determines the angle resolution and the number of detected targets. These are strongly influenced by SA schemes like OES, OUS, NOES, and NOUS. For the total amount of Tx-Rx array of antennas, or the proposed radar with  $M$  and  $N$ , all parameters of SMIMO radar performance are primarily determined by the number of Tx-Rx SAs,  $K$  and  $L$ . The maximum number of targets that can be detected, the SNR detector, the size of the complex amplitude, and the detection probability turn on the number of SAs of the Tx-Rx proposed radar, where the PAR, the MIMO, the PMIMO\_Tx, and the PMIMO\_Tx\_Rx radars represent special schemes. Changing the number of specific  $K$  and  $L$  Tx-Rx SAs ( $M$  and  $N$ ) is adaptive, flexible, and programmable with the proposed radar, providing multi-target detection capabilities with multi-antenna radar systems that increase with target and environment. The condition is more reliable and the design planning radar is easier.




## REFERENCES

- [1] S. Samadi, M. R. Khosravi, J. A. Alzubi, O. A. Alzubi, and V. G. Menon, "Optimum range of angle tracking radars: a theoretical computing," *International Journal of Electrical and Computer Engineering (IJECE)*, vol. 9, no. 3, p. 1765, Jun. 2019, doi: 10.11591/ijece.v9i3.pp1765-1772.
- [2] M. S. Kamal and J. Abdullah, "New algorithm for multi targets detection in clutter edge radar environments," *Indonesian Journal of Electrical Engineering and Computer Science*, vol. 18, no. 1, p. 420, Apr. 2020, doi: 10.11591/ijeecs.v18.i1.pp420-427.
- [3] I. Bilik, O. Longman, S. Villeval, and J. Tabrikian, "The rise of radar for autonomous vehicles: signal processing solutions and future research directions," *IEEE Signal Processing Magazine*, vol. 36, no. 5, pp. 20–31, Sep. 2019, doi: 10.1109/MSP.2019.2926573.
- [4] B. Chauhan, S. C. Gupta, and S. Vijay, "Guard lines conformal slotted antenna array for multiband application," *International Journal of Informatics and Communication Technology (IJ-ICT)*, vol. 10, no. 2, p. 140, Aug. 2021, doi: 10.11591/ijict.v10i2.pp140-147.
- [5] M. Elhefnawy, "Design and simulation of an analog beamforming phased array antenna," *International Journal of Electrical and Computer Engineering (IJECE)*, vol. 10, no. 2, p. 1398, Apr. 2020, doi: 10.11591/ijece.v10i2.pp1398-1405.
- [6] R. C. Hansen, *Phased array antennas*, 2nd ed. Hoboken, NJ, USA: John Wiley & Sons, Inc., 2009.
- [7] D. S. Zmic, G. Zhang, and R. J. Doviak, "Bias correction and doppler measurement for polarimetric phased-array radar," *IEEE Transactions on Geoscience and Remote Sensing*, vol. 49, no. 2, pp. 843–853, Feb. 2011, doi: 10.1109/TGRS.2010.2057436.
- [8] A. Haimovich, R. Blum, and L. Cimini, "MIMO radar with widely separated antennas," *IEEE Signal Processing Magazine*, vol. 25, no. 1, pp. 116–129, 2008, doi: 10.1109/MSP.2008.4408448.
- [9] Y. Li, H. Ma, Y. Wu, L. Cheng, and D. Yu, "DOA estimation for echo signals and experimental results in the AM radio-based passive radar," *IEEE Access*, vol. 6, pp. 73316–73327, 2018, doi: 10.1109/ACCESS.2018.2882304.
- [10] X. Song, N. Zheng, and T. Bai, "Resource allocation schemes for multiple targets tracking in distributed MIMO radar systems," *International Journal of Antennas and Propagation*, vol. 2017, pp. 1–12, 2017, doi: 10.1155/2017/7241281.
- [11] M. Davis, G. Showman, and A. Lanterman, "Coherent MIMO radar: the phased array and orthogonal waveforms," *IEEE Aerospace and Electronic Systems Magazine*, vol. 29, no. 8, pp. 76–91, Aug. 2014, doi: 10.1109/MAES.2014.130148.
- [12] S. Panda, R. Samantaray, P. K. Mohapatra, R. N. Panda, and P. Sahu, "A new complexity reduction methods of V-BLAST MIMO system in a communication channel," *International Journal of Informatics and Communication Technology (IJ-ICT)*, vol. 8, no. 1, p. 29, Apr. 2019, doi: 10.11591/ijict.v8i1.pp29-38.
- [13] A. Hassanien and S. A. Vorobyov, "Phased-MIMO radar: a tradeoff between phased-array and MIMO radars," *IEEE*




- Transactions on Signal Processing*, vol. 58, no. 6, pp. 3137–3151, Jun. 2010, doi: 10.1109/TSP.2010.2043976.
- [14] W. Khan, I. M. Qureshi, A. Basit, and M. Zubair, “Hybrid phased MIMO radar with unequal subarrays,” *IEEE Antennas and Wireless Propagation Letters*, vol. 14, pp. 1702–1705, 2015, doi: 10.1109/LAWP.2015.2419279.
  - [15] S. Tahcfulloh and G. Hendrantoro, “Phased-MIMO radar using Hadamard coded signal,” in *2016 International Conference on Radar, Antenna, Microwave, Electronics, and Telecommunications (ICRAMET)*, Oct. 2016, pp. 13–16, doi: 10.1109/ICRAMET.2016.7849573.
  - [16] A. Alieldin, Y. Huang, and W. M. Saad, “Optimum partitioning of a phased-MIMO radar array antenna,” *IEEE Antennas and Wireless Propagation Letters*, vol. 16, pp. 2287–2290, 2017, doi: 10.1109/LAWP.2017.2714866.
  - [17] M. Hardiwansyah, S. Tahcfulloh, and G. Hendrantoro, “Parameter identifiability of phased-MIMO radar,” in *2019 International Conference of Artificial Intelligence and Information Technology (ICAIIIT)*, Mar. 2019, pp. 192–195, doi: 10.1109/ICAIIIT.2019.8834589.
  - [18] S. Tahcfulloh and G. Hendrantoro, “Full phased MIMO radar with Colocated antennas,” *International Journal on Communications Antenna and Propagation (IRECAP)*, vol. 9, no. 2, p. 144, Apr. 2019, doi: 10.15866/irecap.v9i2.16218.
  - [19] S. Tahcfulloh and G. Hendrantoro, “FPMIMO: a general MIMO structure with overlapping subarrays for various radar applications,” *IEEE Access*, vol. 8, pp. 11248–11267, 2020, doi: 10.1109/ACCESS.2020.2965192.
  - [20] Jian Li, P. Stoica, L. Xu, and W. Roberts, “On parameter identifiability of MIMO radar,” *IEEE Signal Processing Letters*, vol. 14, no. 12, pp. 968–971, Dec. 2007, doi: 10.1109/LSP.2007.905051.
  - [21] E. Fishler, A. Haimovich, R. S. Blum, L. J. Cimini, D. Chizhik, and R. A. Valenzuela, “Spatial diversity in radars—models and detection performance,” *IEEE Transactions on Signal Processing*, vol. 54, no. 3, pp. 823–838, Mar. 2006, doi: 10.1109/TSP.2005.862813.
  - [22] S. Tahcfulloh, “Transmit-receive subarrays for MIMO radar array antenna,” *International Journal on Advanced Science, Engineering and Information Technology*, vol. 11, no. 1, p. 12, Feb. 2021, doi: 10.18517/ijaseit.11.1.10631.
  - [23] S. Tahcfulloh, “MIMO radar array antenna with transmit-receive subarrays,” *International Journal of Intelligent Engineering and Systems*, vol. 13, no. 6, pp. 189–198, Dec. 2020, doi: 10.22266/ijies2020.1231.17.

## BIOGRAPHIES OF AUTHORS



**Syahfrizal Tahcfulloh**    received the B.Eng. degree from Universitas Gadjah Mada, Yogyakarta, Indonesia in 2003, and the M.Eng. and Ph.D. degrees from Institut Teknologi Sepuluh Nopember (ITS), Surabaya, Indonesia in 2010 and 2020, respectively, all in Electrical Engineering. Currently, he is a Lecturer with the Department of Electrical Engineering of Universitas Borneo Tarakan. His research interests include array signal processing and MIMO radar. He is a member of IEEE especially the IEEE Antennas and Propagation Society. He can be contacted at email: rizalubt@gmail.com.



**Muttaqin Hardiwansyah**    is a Lecturer at the Department of Electrical Engineering of Universitas Trunojoyo Madura. He is received the B.Eng. degree from Telecommunication Engineering of Politeknik Elektronika Negeri Surabaya (PENS), Indonesia in 2011, and the M.Eng. degree from Electrical Engineering of Institut Teknologi Sepuluh Nopember (ITS). His research interests include MIMO radar and internet of thing (IoT). He can be contacted at email: muttaqin.hardiwansyah@trunojoyo.ac.id.